

PRECISION TESTS OF THE STANDARD MODEL AND OF THE MINIMAL SUPERSYMMETRIC STANDARD MODEL*

W. HOLLIK

Institut für Theoretische Physik, Universität Karlsruhe
D-76128 Karlsruhe, Germany

(Received November 13, 1996)

The status of the standard model predictions for electroweak precision observables is summarized and the status of the standard model and of the MSSM is discussed in view of the most recent data.

PACS numbers: 12.15. Lk, 12.60. Jv

1. Introduction

By the present high precision experiments stringent tests on the standard model of electroweak and strong interactions are imposed. Impressive achievements have been made in the determination of the Z boson parameters [1], the W mass [2], and the confirmation of the top quark at the Tevatron [3, 4] with mass $m_t = 175 \pm 6$ GeV, but so far direct experimental evidence for the Higgs boson is still lacking.

Also a sizeable amount of theoretical work has contributed over the last few years to a steadily rising improvement of the standard model predictions (for a review see Ref. [5]). The availability of both highly accurate measurements and theoretical predictions provides tests of the quantum structure of the standard model thereby probing the empirically yet unknown Higgs particle via its contribution to the electroweak radiative corrections.

The lack of direct signals from “new physics” makes the high precision experiments also a powerful tool for getting *indirect* information about extensions of the minimal model. Among those, the minimal supersymmetric standard model (MSSM) is the most predictive framework allowing a similarly complete calculation of electroweak precision observables as the standard model.

* Presented at the XXXVI Cracow School of Theoretical Physics, Zakopane, Poland, June 1–11, 1996.

The first part of these lectures covers the present predictions of the standard model and their accuracy, and infers indirect information on the Higgs mass from the recent experimental data. In the second part an equivalent analysis of the electroweak data in the MSSM is presented.

2. Theoretical basis

2.1. Radiative corrections in the standard model

The possibility of performing precision tests is based on the formulation of the standard model as a renormalizable quantum field theory preserving its predictive power beyond tree level calculations. With the experimental accuracy being sensitive to the loop induced quantum effects, also the Higgs sector of the standard model is probed. The higher order terms induce the sensitivity of electroweak observables to the top and Higgs mass m_t, M_H and to the strong coupling constant α_s , which are not present at the tree level.

Before one can make predictions from the theory, a set of independent parameters has to be taken from experiment. For practical calculations the physical input quantities α , G_μ , M_Z , m_f , M_H ; α_s are commonly used for fixing the free parameters of the standard model. Differences between various schemes are formally of higher order than the one under consideration. The study of the scheme dependence of the perturbative results, after improvement by resumming the leading terms, allows us to estimate the missing higher order contributions.

Two fermion induced large loop effects in electroweak observables deserve a special discussion:

- The light fermionic content of the subtracted photon vacuum polarization corresponds to a QED induced shift in the electromagnetic fine structure constant. The recent update of the evaluation of the light quark content [6, 7] yield the result

$$(\Delta\alpha)_{\text{had}} = 0.0280 \pm 0.0007. \quad (1)$$

Other determinations [8] agree within one standard deviation. Together with the leptonic content, $\Delta\alpha$ can be resummed resulting in an effective fine structure constant at the Z mass scale:

$$\alpha(M_Z^2) = \frac{\alpha}{1 - \Delta\alpha} = \frac{1}{128.89 \pm 0.09}. \quad (2)$$

- The electroweak mixing angle is related to the vector boson masses by

$$\sin^2 \theta = 1 - \frac{M_W^2}{M_Z^2} + \frac{M_W^2}{M_Z^2} \Delta\rho + \dots \equiv s_W^2 + c_W^2 \Delta\rho + \dots, \quad (3)$$

where the main contribution to the higher order quantity $\Delta\rho$ is from the (t, b) doublet [9], in 1-loop and neglecting m_b given by:

$$\Delta\rho^{(1)} = 3x_t, \quad x_t = \frac{G_\mu m_t^2}{8\pi^2\sqrt{2}}. \quad (4)$$

Higher order irreducible contributions have become available, modifying $\Delta\rho$ according to

$$\Delta\rho = 3x_t \cdot [1 + x_t \rho^{(2)} + \delta\rho_{\text{QCD}}]. \quad (5)$$

The electroweak 2-loop part [10, 11] is described by the function $\rho^{(2)}(M_H/m_t)$ derived in [11] for general Higgs masses. $\delta\rho_{\text{QCD}}$ is the QCD correction to the leading $G_\mu m_t^2$ term [12, 13]

$$\delta\rho_{\text{QCD}} = -2.86a_s - 14.6a_s^2, \quad a_s = \frac{\alpha_s(m_t)}{\pi}. \quad (6)$$

The Higgs contribution to ρ is only logarithmic for large Higgs masses.

2.2. The vector boson masses

The correlation between the masses M_W, M_Z of the vector bosons in terms of the Fermi constant G_μ , in 1-loop order is given by [14]:

$$\frac{G_\mu}{\sqrt{2}} = \frac{\pi\alpha}{2s_W^2 M_W^2} [1 + \Delta r(\alpha, M_W, M_Z, M_H, m_t)]. \quad (7)$$

The decomposition

$$\Delta r = \Delta\alpha - \frac{c_W^2}{s_W^2} \Delta\rho^{(1)} + (\Delta r)_{\text{remainder}}. \quad (8)$$

separates the leading fermionic contributions $\Delta\alpha$ and $\Delta\rho$. All other terms are collected in the $(\Delta r)_{\text{remainder}}$, the typical size of which is of the order ~ 0.01 .

The presence of large terms in Δr requires the consideration of higher than 1-loop effects. The modification of Eq. (7) according to

$$\begin{aligned} 1 + \Delta r &\rightarrow \frac{1}{(1 - \Delta\alpha) \cdot (1 + \frac{c_W^2}{s_W^2} \Delta\rho) - (\Delta r)_{\text{remainder}}} \\ &\equiv \frac{1}{1 - \Delta r} \end{aligned} \quad (9)$$

accommodates the following higher order terms (Δr in the denominator is an effective correction including higher orders):

- The leading log resummation [15] of $\Delta\alpha$: $1 + \Delta\alpha \rightarrow (1 - \Delta\alpha)^{-1}$
- The resummation of the leading m_t^2 contribution [16] in terms of $\Delta\rho$ in Eq. (5). Beyond the $G_\mu m_t^2 \alpha_s$ approximation through the ρ -parameter, the complete $O(\alpha\alpha_s)$ corrections to the self energies are available from perturbative calculations [17] and by means of dispersion relations [18].
- The recently calculated electroweak 2-loop terms of order $G_\mu m_t^2 M_Z^2$ as part of the remainder [23].
- With the quantity $(\Delta r)_{\text{remainder}}$ in the denominator non-leading higher order terms containing mass singularities of the type $\alpha^2 \log(M_Z/m_f)$ from light fermions are also incorporated [19].

2.3. Z boson observables

With M_Z as a precise input parameter, the predictions for the partial widths as well as for the asymmetries can conveniently be calculated in terms of effective neutral current coupling constants for the various fermions. The effective couplings follow from the set of 1-loop diagrams without virtual photons, the non-QED or weak corrections. These weak corrections can be written in terms of fermion-dependent overall normalizations ρ_f and effective mixing angles s_f^2 in the NC vertices:

$$\begin{aligned} J_\nu^{NC} &= \left(\sqrt{2} G_\mu M_Z^2 \right)^{1/2} (g_V^f \gamma_\nu - g_A^f \gamma_\nu \gamma_5) \\ &= \left(\sqrt{2} G_\mu M_Z^2 \rho_f \right)^{1/2} \left((I_3^f - 2Q_f s_f^2) \gamma_\nu - I_3^f \gamma_\nu \gamma_5 \right). \end{aligned} \quad (10)$$

ρ_f and s_f^2 contain universal parts (i.e. independent of the fermion species) and non-universal parts which explicitly depend on the type of the external fermions. The universal parts arise from the self-energies and contain the Higgs mass dependence. The Higgs contributions to the non-universal vertex corrections are suppressed by the small Yukawa couplings. In their leading terms, incorporating also the next order, the parameters are given by

$$\rho_f = \frac{1}{1 - \Delta\rho} + \dots, \quad s_f^2 = s_W^2 + c_W^2 \Delta\rho + \dots \quad (11)$$

with $\Delta\rho$ from Eq. (6). For the leptonic s_e^2 , the 2-loop contribution $\sim G_\mu m_t^2 M_Z^2$ has become available [23].

For the b quark, also the non-universal parts have a strong dependence on m_t resulting from virtual top quarks in the vertex corrections. The difference between the d and b couplings can be parametrized in the following way

$$\rho_b = \rho_d(1 + \tau)^2, \quad s_b^2 = s_d^2(1 + \tau)^{-1} \quad (12)$$

with the quantity

$$\tau = \Delta\tau^{(1)} + \Delta\tau^{(2)} + \Delta\tau^{(\alpha_s)}$$

calculated perturbatively, at the present level comprising: the complete 1-loop order term [24] with x_t from Eq. (5):

$$\Delta\tau^{(1)} = -2x_t - \frac{G_\mu M_Z^2}{6\pi^2\sqrt{2}}(c_W^2 + 1) \log \frac{m_t}{M_W} + \dots, \quad (13)$$

the leading electroweak 2-loop contribution of $O(G_\mu^2 m_t^4)$ [11, 25]

$$\Delta\tau^{(2)} = -2x_t^2 \tau^{(2)}, \quad (14)$$

where $\tau^{(2)}$ is a function of M_H/m_t with $\tau^{(2)} = 9 - \pi^2/3$ for $M_H \ll m_t$; the QCD corrections to the leading term of $O(\alpha_s G_\mu m_t^2)$ [26]

$$\Delta\tau^{(\alpha_s)} = 2x_t \cdot \frac{\alpha_s}{\pi} \cdot \frac{\pi^2}{3}, \quad (15)$$

and the $O(\alpha_s)$ correction to the $\log m_t/M_W$ term in (17), with a numerically very small coefficient [27].

Asymmetries and mixing angles: The effective mixing angles are of particular interest since they determine the on-resonance asymmetries via the combinations

$$A_f = \frac{2g_V^f g_A^f}{(g_V^f)^2 + (g_A^f)^2}. \quad (16)$$

Measurements of the asymmetries hence are measurements of the ratios

$$g_V^f/g_A^f = 1 - 2Q_f s_f^2 \quad (17)$$

or of the effective mixing angles, respectively.

The measurable quantities are:

— the forward backward asymmetries in $e^+e^- \rightarrow f\bar{f}$:

$$A_{FB} = \frac{3}{4} A_e \cdot A_f$$

— the left-right asymmetry:

$$A_{LR} = A_e$$

— the τ polarization in $e^+e^- \rightarrow \tau^+\tau^-$:

$$P_\tau = A_\tau.$$

Z width and partial widths: The total Z width Γ_Z can be calculated essentially as the sum over the fermionic partial decay widths

$$\Gamma_Z = \sum_f \Gamma_f + \dots, \quad \Gamma_f = \Gamma(Z \rightarrow f\bar{f}). \quad (18)$$

The dots indicate other decay channels which, however, are not significant. The fermionic partial widths, when expressed in terms of the effective coupling constants read up to 2nd order in the fermion masses:

$$\Gamma_f = \Gamma_0 \left((g_V^f)^2 + (g_A^f)^2 \left(1 - \frac{6m_f^2}{M_Z^2}\right) \right) \cdot (1 + Q_f^2 \frac{3\alpha}{4\pi}) + \Delta\Gamma_{\text{QCD}}^f$$

with

$$\Gamma_0 = N_C^f \frac{\sqrt{2}G_\mu M_Z^3}{12\pi}, \quad N_C^f = 1 \text{ (leptons)}, = 3 \text{ (quarks)}$$

and the QCD corrections $\Delta\Gamma_{\text{QCD}}^f$ for quark final states [20]. The QCD correction for the light quarks with $m_q \simeq 0$ is given by

$$\Delta\Gamma_{\text{QCD}}^f = \Gamma_0 \left((g_V^f)^2 + (g_A^f)^2 \right) \cdot K_{\text{QCD}} \quad (19)$$

with [28]

$$K_{\text{QCD}} = \frac{\alpha_s}{\pi} + 1.41 \left(\frac{\alpha_s}{\pi} \right)^2 - 12.8 \left(\frac{\alpha_s}{\pi} \right)^3 - \frac{Q_f^2}{4} \frac{\alpha\alpha_s}{\pi^2}.$$

For b quarks the QCD corrections are different due to finite b mass terms and to top quark dependent 2-loop diagrams for the axial part:

$$\Delta\Gamma_{\text{QCD}}^b = \Delta\Gamma_{\text{QCD}}^d + \Gamma_0 \left[(g_V^b)^2 R_V + (g_A^b)^2 R_A \right]. \quad (20)$$

The coefficients in the perturbative expansions

$$R_V = c_1^V \frac{\alpha_s}{\pi} + c_2^V \left(\frac{\alpha_s}{\pi} \right)^2 + c_3^V \left(\frac{\alpha_s}{\pi} \right)^3 + \dots,$$

$$R_A = c_1^A \frac{\alpha_s}{\pi} + c_2^A \left(\frac{\alpha_s}{\pi} \right)^2 + \dots$$

depending on m_b and m_t , are calculated up to third order in the vector and up to second order in the axial part [29].

2.4. Accuracy of the standard model predictions

For a discussion of the theoretical reliability of the standard model predictions one has to consider the various sources contributing to their uncertainties:

The experimental error of the hadronic contribution to $\alpha(M_Z^2)$, Eq. (2), leads to $\delta M_W = 13$ MeV in the W mass prediction, and $\delta \sin^2 \theta = 0.00023$ common to all of the mixing angles, which matches with the experimental precision.

The uncertainties from the QCD contributions, besides the 3 MeV in the hadronic Z width, can essentially be traced back to those in the top quark loops for the ρ -parameter. They can be combined into the following errors [21]:

$$\delta(\Delta\rho) \simeq 1.5 \cdot 10^{-4}, \quad \delta s_\ell^2 \simeq 0.0001$$

for $m_t = 175$ GeV.

TABLE I

Largest half-differences among central values (Δ_c) and among maximal and minimal predictions (Δ_g) for $m_t = 175$ GeV, $60 \text{ GeV} < M_H < 1 \text{ TeV}$, $\alpha_s(M_Z^2) = 0.125$ (from Ref. [22])

Observable O	$\Delta_c O$	$\Delta_g O$
M_W (GeV)	4.5×10^{-3}	1.6×10^{-2}
Γ_e (MeV)	1.3×10^{-2}	3.1×10^{-2}
Γ_Z (MeV)	0.2	1.4
s_e^2	5.5×10^{-5}	1.4×10^{-4}
s_b^2	5.0×10^{-5}	1.5×10^{-4}
R_{had}	4.0×10^{-3}	9.0×10^{-3}
R_b	6.5×10^{-5}	1.7×10^{-4}
R_c	2.0×10^{-5}	4.5×10^{-5}
σ_0^{had} (nb)	7.0×10^{-3}	8.5×10^{-3}
A_{FB}^l	9.3×10^{-5}	2.2×10^{-4}
A_{FB}^e	3.0×10^{-4}	7.4×10^{-4}
A_{FB}^τ	2.3×10^{-4}	5.7×10^{-4}
A_{LR}	4.2×10^{-4}	8.7×10^{-4}

The size of unknown higher order contributions can be estimated by different treatments of non-leading terms of higher order in the implementation of radiative corrections in electroweak observables ('options') and by investigations of the scheme dependence. Explicit comparisons between the results of 5 different computer codes based on on-shell and \overline{MS} calculations for the Z resonance observables are documented in the "Electroweak

Working Group Report" [22] in Ref. [5]. Table 1 shows the uncertainty in a selected set of precision observables. Quite recently (not included in Table I) the non-leading 2-loop corrections $\sim G_\mu^2 m_t^2 M_Z^2$ have been calculated [23] for Δr and s_ℓ^2 . They reduce the uncertainty in M_W and s_ℓ^2 considerably, by about a factor 0.2.

3. Standard model and precision data

In Table II the standard model predictions for Z pole observables and the W mass are put together for a light and a heavy Higgs particle with $m_t = 175$ GeV. The last column is the variation of the prediction according to $\Delta m_t = \pm 6$ GeV. The input value $\alpha_s = 0.123$ is the one from QCD observables at the Z peak [30]. Not included are the uncertainties from $\delta\alpha_s = 0.006$, which amount to 3 MeV for the hadronic Z width. The experimental results on the Z observables are from combined LEP and SLD data. ρ_ℓ and s_ℓ^2 are the leptonic neutral current couplings in Eq. (10), derived from partial widths and asymmetries under the assumption of lepton universality. The table illustrates the sensitivity of the various quantities to the Higgs mass. The effective mixing angle turns out to be the most sensitive observable, where both the experimental error and the uncertainty from m_t are small compared to the variation with M_H . Since a light Higgs boson goes along with a low value of s_ℓ^2 , the strongest upper bound on M_H is from A_{LR} at the SLC [31], whereas LEP data alone allow to accommodate also a relatively heavy Higgs (see figure 1). Further constraints on M_H are to be expected in the future from more precise M_W measurements at LEP 2.

TABLE II

Precision observables: experimental results [1] and standard model predictions.

observable	exp. (1996)	$M_H = 65$ GeV	$M_H = 1$ TeV	Δm_t
M_Z (GeV)	91.1863 ± 0.0020	input	input	
Γ_Z (GeV)	2.4946 ± 0.0027	2.5015	2.4923	± 0.0015
σ_0^{had} (nb)	41.508 ± 0.056	41.441	41.448	± 0.003
$\Gamma_{\text{had}}/\Gamma_e = R_e$	20.778 ± 0.029	20.798	20.770	± 0.002
$\Gamma_b/\Gamma_{\text{had}} = R_b$	0.2178 ± 0.0011	0.2156	0.2157	± 0.0002
$\Gamma_c/\Gamma_{\text{had}} = R_c$	0.1715 ± 0.0056	0.1724	0.1723	± 0.0001
A_b	0.867 ± 0.022	0.9350	0.9340	± 0.0001
ρ_ℓ	1.0043 ± 0.0014	1.0056	1.0036	± 0.0006
s_ℓ^2	0.23165 ± 0.00024	0.23115	0.23265	± 0.0002
M_W (GeV)	80.356 ± 0.125	80.414	80.216	± 0.038

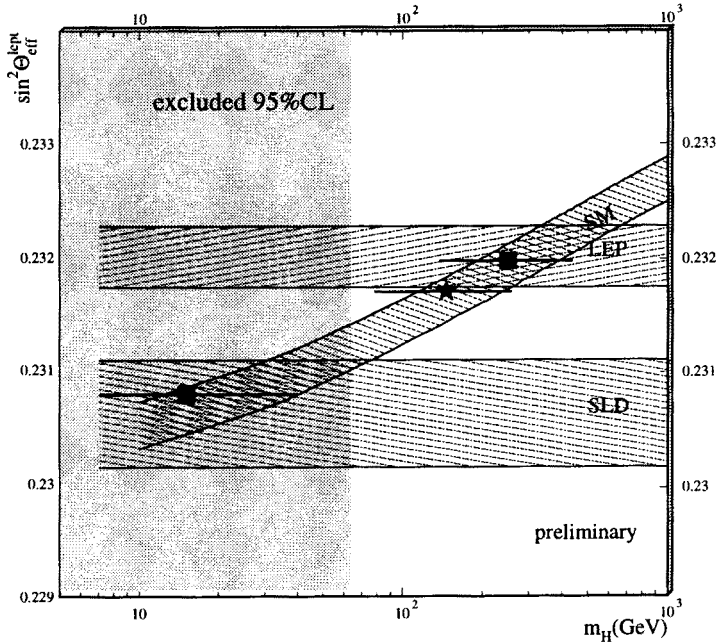


Fig. 1. Dependence of the leptonic mixing angle on the Higgs mass. The theoretical predictions correspond to $m_t = 175 \pm 6$ GeV. The SLD [31] (0.23061 ± 0.00047) and LEP [1] (0.23200 ± 0.00027) measurements are separately shown. The star is the result of a combined fit to LEP and SLD data, the squares are for separate fits (from Ref. [33]).

Besides the direct measurement of the W mass, the quantity s_W^2 resp. the ratio M_W/M_Z is indirectly measured in deep-inelastic neutrino scattering, in particular in the NC/CC neutrino cross section ratio for isoscalar targets. The world average [1] from CCFR, CDHS and CHARM, including the new CCFR result [32]

$$s_W^2 = 1 - M_W^2/M_Z^2 = 0.2244 \pm 0.0044$$

is fully consistent with the direct vector boson mass measurements.

Standard model fits and Higgs mass range: Assuming the validity of the standard model a global fit to all electroweak results from LEP, SLD, M_W , νN and m_t , allows to derive information on the allowed range for the Higgs mass.

Although the Higgs mass dependence of the electroweak parameters is only logarithmic, the already quite accurate value for m_t leads to some

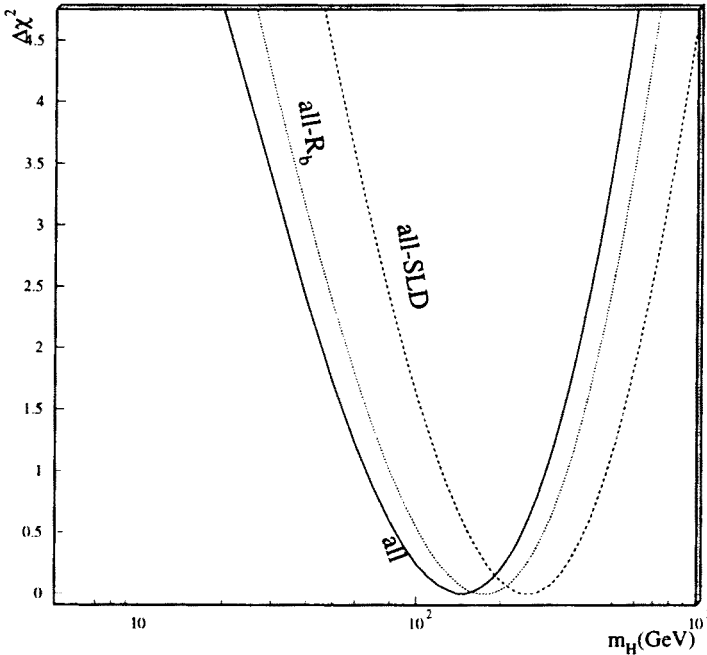


Fig. 2. Dependence of $\Delta\chi^2 = \chi^2 - \chi_{min}^2$ on the Higgs mass (from Ref. [33]).

sensitivity to M_H . The Higgs mass dependence of the χ^2 of an overall fit is shown in figure 2 [33]. As one can see, the impact of R_b , which is on the way to the standard model value, is only marginal whereas A_{LR} is decisive for a restrictive upper bound for M_H . From the fit one obtains [1, 33]:

$$M_H = 149_{-82}^{+148} \text{ GeV}, \quad M_H < 450 \text{ GeV} (95\% \text{ C.L.}).$$

Similar results have been obtained in [35, 36] (updated from [37]). Without A_{LR} , the 95% C.L upper bound is shifted upwards by about 260 GeV.

These numbers do not yet include the theoretical uncertainties of the standard model predictions. The LEP-EWWG [1, 34] has performed a study of the influence of the various 'options' discussed in section 2.4 on the bounds for the Higgs mass with the result that the 95% C.L. upper bound is shifted by +100 GeV to higher values. It has to be kept in mind, however, that this error estimate is based on the uncertainties as given in Table I. Since the recent improvement in the theoretical prediction [23] is going to reduce the theoretical uncertainty especially in the effective mixing angle one may expect also a significant smaller theoretical error on the Higgs mass bounds once the 2-loop terms $\sim G_\mu^2 m_t^2 M_Z^2$ are implemented in the codes used for the fits. At the present stage the codes are without the new terms.

4. Precision tests of the MSSM

4.1. MSSM entries

The MSSM deserves a special discussion as the most predictive framework beyond the minimal model. Its structure allows a similarly complete calculation of the electroweak precision observables as in the standard model in terms of one Higgs mass (usually taken as M_A) and $\tan\beta = v_2/v_1$, together with the set of SUSY soft breaking parameters fixing the chargino/neutralino and scalar fermion sectors. It has been known since quite some time [38] that light non-standard Higgs bosons as well as light stop and charginos predict larger values for the ratio R_b [39, 41] (see figures 3, 4). Complete 1-loop calculations are available for Δr [40] and for the Z boson observables [41].

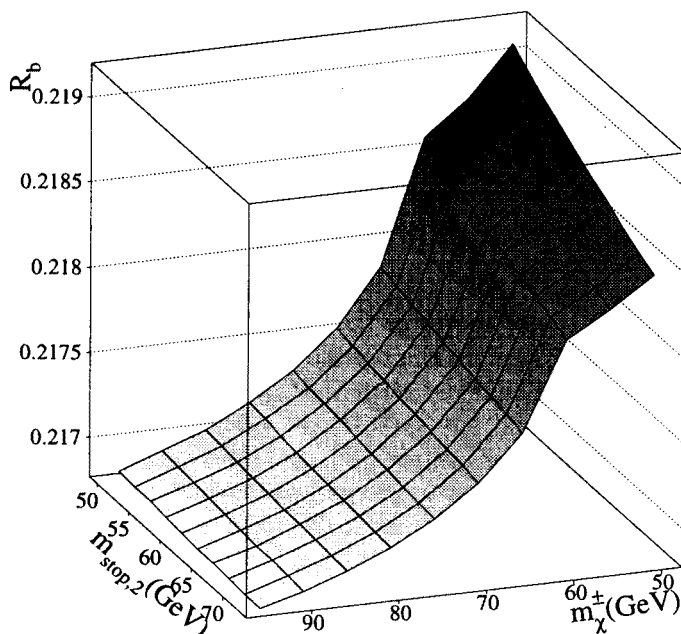


Fig. 3. R_b in the light stop-chargino plane. $\tan\beta = 1.6$ [33].

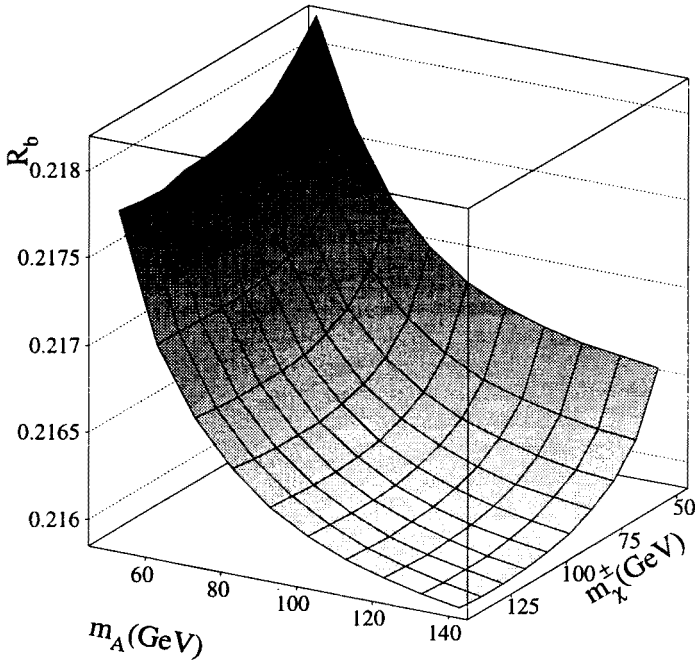


Fig. 4. R_b in the pseudoscalar Higgs-chargino plane $\tan \beta = 34$ [33].

Higgs sector: The scalar sector of the MSSM is completely determined by the value of $\tan \beta = v_2/v_1$ and the pseudoscalar mass M_A , together with the radiative corrections. The latter ones are taken into account in terms of the effective potential approximation with the leading terms $\sim m_t^4$, including the mixing in the scalar top system [42]. In this way, the coupling constants of the various Higgs particles to gauge bosons and fermions can be taken over from [43] substituting only the scalar mixing angle α by the improved effective mixing angle which is obtained from the diagonalization of the scalar mass matrix.

Sfermion sector: The physical masses of squarks and sleptons are given by the eigenvalues of the 2×2 mass matrix:

$$\mathcal{M}_f^2 = \begin{pmatrix} M_{\tilde{Q}}^2 + m_f^2 + M_Z^2(I_3^f - Q_f s_W^2) \cos 2\beta & m_f(A_f + \mu\{\cot\beta, \tan\beta\}) \\ m_f(A_f + \mu\{\cot\beta, \tan\beta\}) & M_{\{\tilde{U}, \tilde{D}\}}^2 + m_f^2 + M_Z^2 Q_f s_W^2 \cos 2\beta \end{pmatrix} \quad (21)$$

with SUSY soft breaking parameters $M_{\tilde{Q}}$, $M_{\tilde{U}}$, $M_{\tilde{D}}$, A_f , and μ . It is convenient to use the following notation for the off-diagonal entries in Eq. (21):

$$A'_f = A_f + \mu\{\cot\beta, \tan\beta\}. \quad (22)$$

Scalar neutrinos appear only as left-handed mass eigenstates. Up and down type sfermions in (21) are distinguished by setting $f = u, d$ and the $\{u, d\}$ entries in the parenthesis. Since the non-diagonal terms are proportional to m_f , it seems natural to assume unmixed sfermions for the lepton and quark case except for the scalar top sector. The \tilde{t} mass matrix is diagonalized by a rotation matrix with a mixing angle Φ_{mix} . Instead of $M_{\tilde{Q}}$, $M_{\tilde{U}}$, $M_{\tilde{D}}$, A'_t for the \tilde{b} , \tilde{t} system the physical squark masses $m_{\tilde{b}_L}$, $m_{\tilde{b}_R}$, $m_{\tilde{t}_2}$ can be used together with A'_t or, alternatively, the stop mixing angle Φ_{mix} . For simplicity we assume $m_{\tilde{b}_L} = m_{\tilde{b}_R}$, and \tilde{u} , \tilde{d} , \tilde{c} , \tilde{s} to have masses equal to the \tilde{b} squark mass.

A possible mass splitting between \tilde{b}_L - \tilde{t}_L yields a contribution to the ρ -parameter $\rho = 1 + \Delta\rho$ in terms of ¹

$$\Delta\rho_{\tilde{b}-\tilde{t}}^0 = \frac{3G_\mu}{8\pi^2\sqrt{2}} \left(m_{\tilde{b}_L}^2 + m_{\tilde{t}_L}^2 - 2 \frac{m_{\tilde{b}_L}^2 m_{\tilde{t}_L}^2}{m_{\tilde{b}_L}^2 - m_{\tilde{t}_L}^2} \log \frac{m_{\tilde{b}_L}^2}{m_{\tilde{t}_L}^2} \right). \quad (23)$$

As a universal loop contribution, it enters the quantity Δr and the Z boson couplings through the relations (8) and (11) and is thus significantly constrained by the data on M_W and the leptonic widths.

Chargino/Neutralino sector: The chargino (neutralino) masses and the mixing angles in the gaugino couplings are calculated from soft breaking parameters M_1 , M_2 and μ in the chargino (neutralino) mass matrix [43]. For practical calculations, the GUT relation $M_1 = 5/3 \tan^2 \theta_W M_2$ is conventionally assumed.

The chargino 2×2 mass matrix is given by

$$\mathcal{M}_{\tilde{\chi}^\pm} = \begin{pmatrix} M_2 & M_W \sqrt{2} \sin \beta \\ M_W \sqrt{2} \cos \beta & -\mu \end{pmatrix}, \quad (24)$$

¹ The superscript $\Delta\rho^0$ indicates that no left-right mixing is included.

with the SUSY soft breaking parameters μ and M_2 in the diagonal matrix elements. The physical chargino mass states $\tilde{\chi}_i^\pm$ are the rotated wino and charged Higgsino states:

$$\begin{aligned}\tilde{\chi}_i^+ &= V_{ij}\psi_j^+ \\ \tilde{\chi}_i^- &= U_{ij}\psi_j^- ; i, j = 1, 2 .\end{aligned}\quad (25)$$

V_{ij} and U_{ij} are unitary chargino mixing matrices obtained from the diagonalization of the mass matrix Eq. (24):

$$U^* \mathcal{M}_{\tilde{\chi}^\pm} V^{-1} = \text{diag}(m_{\tilde{\chi}_1^\pm}, m_{\tilde{\chi}_2^\pm}) . \quad (26)$$

The neutralino 4×4 mass matrix can be written as:

$$\mathcal{M}_{\tilde{\chi}^0} = \begin{pmatrix} M_1 & 0 & -M_Z \sin \theta_W \cos \beta & M_Z \sin \theta_W \sin \beta \\ 0 & M_2 & M_Z \cos \theta_W \cos \beta & -M_Z \cos \theta_W \sin \beta \\ -M_Z \sin \theta_W \cos \beta & M_Z \cos \theta_W \cos \beta & 0 & \mu \\ M_Z \sin \theta_W \sin \beta & -M_Z \cos \theta_W \sin \beta & \mu & 0 \end{pmatrix} \quad (27)$$

where the diagonalization can be obtained by the unitary matrix N_{ij} :

$$N^* \mathcal{M}_{\tilde{\chi}^0} N^{-1} = \text{diag}(m_{\tilde{\chi}_i^0}) . \quad (28)$$

The elements U_{ij} , V_{ij} , N_{ij} of the diagonalization matrices enter the couplings of the charginos, neutralinos and sfermions to fermions and gauge bosons, as explicitly given in Ref. [43]. Note that our sign convention on the parameter μ is opposite to that of Ref. [43].

4.2. MSSM global fits

For obtaining the optimized SUSY parameter set a global fit to all the electroweak precision data, including the top mass measurement, has been performed [33] with the new data. The essential features are: The difference between the experimental and the SM value of R_b can now be fully explained by the MSSM. Other quantities are practically unchanged. In total, the χ^2 of the fit is slightly better than in the standard model, but due to the larger numbers of parameters, the probability for the standard model is higher. A similar situation occurs for large $\tan \beta$ with light Higgs bosons h^0, A^0 not far above 50 GeV.

In order to obtain the best MSSM fits the precision data in Table IV were taken into account together with the error correlations, the measurement of

TABLE III

Mass limits assumed for the optimized fits

experimental limits	
$\tilde{m}_{\chi_{1,2}^\pm}$	$> 65 \text{ GeV}$
$\tilde{m}_{\chi_1^0}$	$> 13 \text{ GeV}$
$\tilde{m}_{\chi_2^0}$	$> 35 \text{ GeV}$
$\tilde{m}_{\chi_{3,4}^0}$	$> 60 \text{ GeV}$
$\Gamma_{Z \rightarrow \text{neutralinos}}$	$< 2 \text{ MeV}$
$\tilde{m}_{t_{1,2}}$	$> 48 \text{ GeV}$
m_h, m_H, m_A, m_{H^\pm}	$> 50 \text{ GeV}$

TABLE IV

Measurements[1] and the predicted results of the fits with minimum χ^2 (Ref. [33]). The pulls are defined by (measurement - predicted value) / error of the measurement.

Symbol		measurement	best fit observables						
			SM		MSSM				
tan β and pull			pull		1.6	pull		34	pull
M_Z [GeV]	91.1863 \pm 0.0020	91.1861	0.08	91.1863	0.00	91.1863	0.00		
Γ_Z [GeV]	2.4946 \pm 0.0027	2.4959	-0.49	2.4946	0.00	2.4939	0.24		
σ_h [nb]	41.508 \pm 0.056	41.466	0.75	41.4607	0.84	41.449	1.06		
R_e	20.778 \pm 0.029	20.756	0.74	20.7690	0.31	20.772	0.21		
A_{FB}^l	0.0174 \pm 0.0010	0.0159	1.48	0.0162	1.22	0.0161	1.25		
R_b	0.2178 \pm 0.0011	0.2158	1.75	0.2173	0.42	0.2167	0.96		
R_c	0.1715 \pm 0.0056	0.1723	-0.14	0.1707	0.14	0.1709	0.12		
A_{FB}^b	0.0979 \pm 0.0023	0.1020	-1.77	0.1030	-2.22	0.1030	-2.19		
A_{FB}^c	0.0735 \pm 0.0048	0.0729	0.12	0.0736	-0.01	0.0735	0.01		
\mathcal{A}_b	0.863 \pm 0.049	0.933	-1.45	0.935	-1.49	0.936	-1.50		
\mathcal{A}_c	0.625 \pm 0.084	0.667	-0.50	0.668	-0.51	0.668	-0.51		
\mathcal{A}_τ	0.1401 \pm 0.0067	0.1457	-0.83	0.1469	-1.01	0.1464	-0.95		
\mathcal{A}_e	0.1382 \pm 0.0076	0.1457	-0.99	0.1469	-1.14	0.1467	-1.12		
$\sin^2 \theta_e(Q_{FB})$	0.2320 \pm 0.0010	0.2317	0.31	0.2315	0.46	0.2316	0.44		
M_W [GeV]	80.356 \pm 0.125	80.353	0.03	80.401	-0.36	80.425	-0.55		
$1-M_W^2/M_Z^2$	0.2244 \pm 0.0042	0.2235	0.21	0.2226	0.44	0.2221	0.55		
m_t [GeV]	175 \pm 6.	172.2	0.46	172.3	0.46	171.9	0.514		
$\sin^2 \theta_e(A_{LR})$	0.23061 \pm 0.00047	0.2317	-2.16	0.2315	-1.86	0.2316	-1.89		

TABLE V

Values of the fitted parameters (upper part) and corresponding mass spectrum (lower part). The errors on the parameters are parabolic ones. On the right hand side the results of the optimization for high $\tan \beta$ are given. In this case $\tan \beta$ was left free and resulted in $\tan \beta \approx 34$. The dashes indicate irrelevant parameters which were chosen high. (From [33]).

Fitted SUSY parameters and masses		
Symbol	$\tan \beta = 1.6$	$\tan \beta = 34$
	$b \rightarrow s\gamma$ inc.	
m_t [GeV]	172 ± 5	172 ± 5
α_s	0.116 ± 0.005	0.1190 ± 0.005
M_2 [GeV]	116^{+146}_{-18}	-
μ [GeV]	61^{+51}_{-61}	112 ± 386
$m_{\tilde{t}_2}$ [GeV]	49^{+68}_{-7}	238 ± 473
ϕ_{mix}	-0.18 ± 0.08	0.05 ± 0.06
m_A [GeV]	-	50 ± 5
Particle Spectrum		
$m_{\tilde{t}_1}$ [GeV]	≈ 1 TeV	
$m_{\tilde{t}_2}$ [GeV]	49	238
$m_{\tilde{q}}$ [GeV]	1 TeV	
$m_{\tilde{l}}$ [GeV]	0.5 TeV	
$m_{\tilde{\chi}_1^\pm}$ [GeV]	151	1504
$m_{\tilde{\chi}_2^\pm}$ [GeV]	85	112
$m_{\tilde{\chi}_1^0}$ [GeV]	55	109
$m_{\tilde{\chi}_2^0}$ [GeV]	66	116
$m_{\tilde{\chi}_3^0}$ [GeV]	101	716
$m_{\tilde{\chi}_4^0}$ [GeV]	152	1504
m_h [GeV]	109	50
m_H [GeV]	≈ 1.5 TeV	115
m_A [GeV]	1.5 TeV	50
m_{H^\pm} [GeV]	≈ 1.5 TeV	122
M_W^\pm [GeV]	80.401	80.425
$\frac{BR(b \rightarrow s\gamma)}{BR(b \rightarrow ce\bar{\nu})}/10^{-4}$	2.42	2.33
$\chi^2/d.o.f.$	16.1/12	17.7/11
Probability	19%	9%

the branching ratio $BR(b \rightarrow s\gamma)$ by CLEO [46], and the experimental limits on the masses of non-standard particles from LEP and Tevatron [47, 48], as given in Table III. The calculation of the total decay width of the Z boson into neutralinos is based on Ref. [44], the calculation of the ratio $b \rightarrow s\gamma$ on Ref. [45].

R_b increases with decreasing $\tan\beta$, but the $b \rightarrow s\gamma$ rate becomes too small if $\tan\beta$ is near one. With $b \rightarrow s\gamma$ included in the fit and a free $\tan\beta$, the preferred value of $\tan\beta$ was either around 1.6 or 34.

The fit results for these values of $\tan\beta$ are given in Table V and the predicted values of all observables with their pulls have been summarized in Table IV. Note that the MSSM prediction of the W -boson mass is always higher than the Standard Model one, but the values of the strong coupling constant and the top mass are very similar in the MSSM:

$$\alpha_s(M_Z) = 0.116 \pm 0.005$$

$$m_t = 172 \pm 5 \text{ GeV}.$$

These values are for the low $\tan\beta$ scenario. For high $\tan\beta$ the same values are obtained, except for $\alpha_s = 0.119 \pm 0.005$ in that case. The remaining parameters are given in Table V. The Higgs mass is not an independent parameter in the MSSM, since the couplings in the Higgs potential are gauge couplings, which limit the mass of the lightest Higgs to a rather narrow range[49]. The high $\tan\beta$ scenario needs a light pseudoscalar Higgs mass, practically degenerate with the light scalar mass.

For the best solutions the gluino mass was fixed to 1500 GeV, the $\tilde{\tau}$ mass to 500 GeV and the sbottom mass to 1000 GeV in both the low and the high $\tan\beta$ scenario, since they are less sensitive to the LEP observables and therefore cannot be fitted. Their influence was studied by fixing them to different values and repeating the fits again. First the low $\tan\beta$ scenario will be discussed. A variation of the gluino mass from 200 GeV up to 2000 GeV did not change the best obtainable χ^2 , varying the $\tilde{\tau}$ mass in the same range changed the χ^2 less than 0.2. Furthermore, the best obtainable χ^2 changed less than 0.2 when varying the sbottom mass and pseudoscalar Higgs mass from 800 GeV to 2000 GeV. For values of these two parameters below 800 GeV the χ^2 increased significantly, mainly because the prediction of R_b became too small.

Within the high $\tan\beta$ scenario no significant change of the global χ^2 was detected when the gluino mass was varied between 200 GeV and 2000 GeV, but the $\tilde{\tau}$ mass was somewhat more sensitive. A variation of this parameter between 300 GeV and 700 GeV changed the global χ^2 less than 0.2, but if it was chosen higher than 1000 GeV the χ^2 increased up to 1.6 units, mainly because the prediction of \mathcal{A}_τ became worse. The sbottom mass was varied between 800 GeV and 2000 GeV. As in the low $\tan\beta$ case there was

no dependence on this parameter if it was chosen heavy, but for low values the preferred top mass became too small. M_2 was fixed at 1500 GeV. A variation between 1000 GeV and 2000 GeV changed the best reachable χ^2 less than 0.2, for smaller values the global χ^2 increased up to one unit. Note that $\tan\beta$ was left as a free parameter in this case.

To check the influence of the assumptions on M_1 for the best fits, the GUT relation $M_1 = 5/3 \tan^2\theta_W M_2$ was dropped and the fit was repeated with a free M_1 , but this did not improve the best obtainable χ^2 significantly.

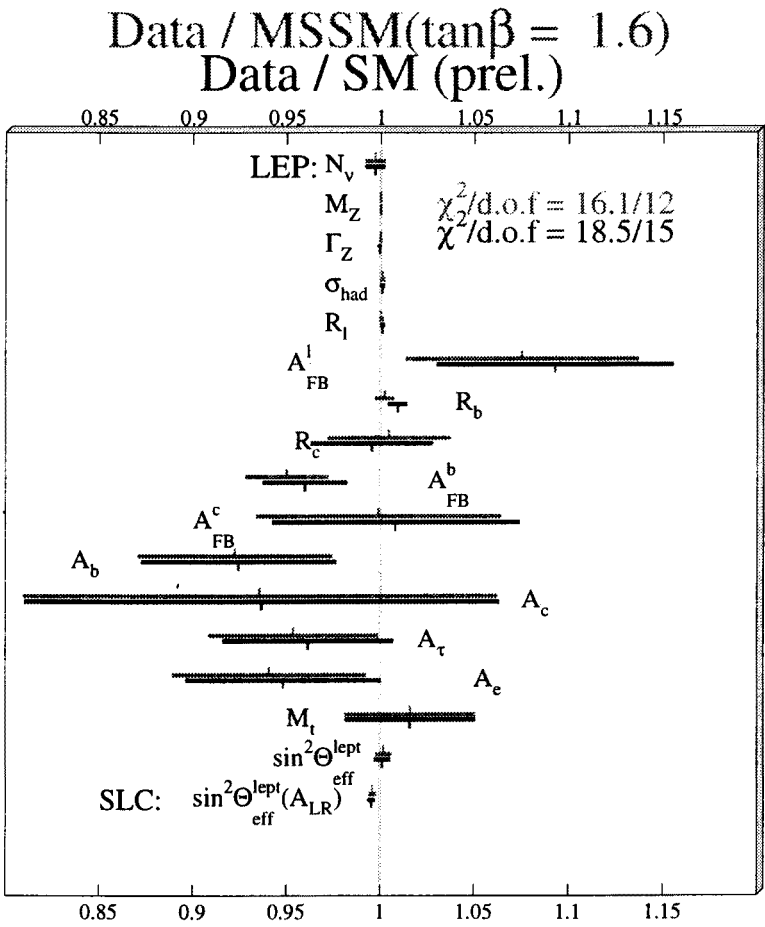


Fig. 5. Experimental data normalized to the best fit results in the SM and MSSM [33].

A direct comparison to the Standard Model fits is shown in figure 5 for $\tan\beta = 1.6$; a very similar plot is obtained for $\tan\beta = 34$. The resulting Standard Model $\chi^2/d.o.f. = 18.5/15$ corresponds to a probability of 24%, the MSSM fits correspond to probabilities of 19% ($\tan\beta = 1.6$, $\chi^2/d.o.f. = 16.1/12$) and 9% ($\tan\beta=34$, $\chi^2/d.o.f. = 17.7/11$). In counting the d.o.f the insensitive (and fixed) parameters were ignored. Although the global χ^2 of the fits can be improved and the remaining discrepancy in R_b can be fully explained if Supersymmetry is assumed, both the high and the low $\tan\beta$ scenario have a lower probability than the SM, because of the larger number of free parameters in MSSM. Therefore, from the point of view of electroweak precision measurements there is no compelling need for Supersymmetrie, in agreement with results from Ref. [35].

Another interesting point is the fitted value of $\alpha_s(M_Z)$. In previous analysis with the high values of R_b $\alpha_s(M_Z)$ in the MSSM (≈ 0.11) was always significantly smaller than the SM value (0.123 ± 0.005 [48]), which supported the low energy values from deep inelastic scattering (DIS) (0.112 ± 0.005 [48]) and lattice calculations of the heavy quark splittings (0.110 ± 0.006 [48]). However, the discrepancies between the low energy α_s values and the LEP data have practically disappeared at the Warsaw Conference [50]: the Standard Model value (0.120 ± 0.003 , see above) is now in agreement with DIS measurements (0.115 ± 0.005 [50]), lattice calculations 0.117 ± 0.003 [50] and the world average 0.118 ± 0.003 [50]. The MSSM values of α_s are in good agreement with these other determinations.

The particle spectrum for the best fits suggests that some SUSY particles could be within reach of LEP 2. The χ^2 in the region of the best low $\tan\beta$ fit increases slowly for increasing chargino masses. Chargino masses above a possible LEP 2 limit of 95 GeV will increase the global χ^2 of the fit by approximately 2 units, which decreases the probability from 19 to 11%.

The best $\tan\beta = 1.6$ fit has a light stop mass of about 49 GeV, and the lightest neutralino is about 55 GeV, so this solution is not excluded by stop searches at LEP1 and the Tevatron.

Within the high $\tan\beta$ scenario both neutral h^0, A^0 bosons are light and have practically the same mass. This scenario can safely be excluded if no Higgs bosons will be found at LEP 2.

5. Conclusions

In view of the recent data, the standard model is in a good shape. By its quantum structure the mass of the as yet experimentally unknown Higgs boson can be probed through its contribution to the radiative corrections for electroweak precision observables. The present upper bound on M_H is

dominated by the result on A_{LR} . The instability of the Higgs mass range obtained from global fits with or without A_{LR} recommends to consider the present mass bound with some caution. The only safe conclusion is that we are well below the critical range where the standard Higgs becomes non-perturbative.

The MSSM also provides a good description of all electroweak data and is competitive to the standard model. The best MSSM fit with light stop and light charginos is obtained for $\tan \beta = 1.6$. Although the MSSM can fully explain the remaining deviation of R_b from the SM value, its probability is not better because of the larger number of free parameters.

I want to thank Marek Jeżabek and the organizers for the invitation and for the kind hospitality at Zakopane.

REFERENCES

- [1] A. Blondel, ICHEP96 (plenary talk), Warsaw, July 1996.
- [2] M. Rijssenbeck, ICHEP96 (talk), Warsaw, July 1996.
- [3] CDF Collaboration, F. Abe *et al.*, *Phys. Rev. Lett.* **74**, 2626 (1995); D0 Collaboration, S. Abachi *et al.*, *Phys. Rev. Lett.* **74**, 2632 (1995);
- [4] P. Tipton, ICHEP96 (plenary talk); P. Grannis, ICHEP96 (talk), Warsaw, July 1996.
- [5] Reports of the Working Group on Precision Calculations for the Z Resonance, CERN 95-03 (1995), Eds. D. Bardin, W. Hollik, G. Passarino
- [6] S. Eidelman, F. Jegerlehner, *Z. Phys.* **C67**, 585 (1995).
- [7] H. Burkhardt, B. Pietrzyk, *Phys. Lett.* **B356**, 398 (1995).
- [8] M.L. Swartz, *Phys. Rev.* **D53**, 5268 (1996); A.D. Martin, D. Zeppenfeld, *Phys. Lett.* **B345**, 558 (1995); K. Adel, F.J. Yndurain, hep-ph/9509378; D.H. Brown, W.A. Worstell, hep-ph/9607319.
- [9] M. Veltman, *Nucl. Phys.* **B123**, 89 (1977); M.S. Chanowitz, M.A. Furman, I. Hinchliffe, *Phys. Lett.* **B78**, 285 (1978).
- [10] J.J. van der Bij, F. Hoogeveen, *Nucl. Phys.* **B283**, 477 (1987).
- [11] R. Barbieri, M. Beccaria, P. Ciafaloni, G. Curci, A. Vicere, *Phys. Lett.* **B288** (1992) 95; *Nucl. Phys.* **B409**, 105 (1993); J. Fleischer, F. Jegerlehner, O.V. Tarasov, *Phys. Lett.* **B319**, 249 (1993).
- [12] A. Djouadi, C. Verzegnassi, *Phys. Lett.* **B195**, 265 (1987).
- [13] L. Avdeev, J. Fleischer, S.M. Mikhailov, O. Tarasov, *Phys. Lett.* **B336**, 560 (1994); *E: Phys. Lett.* **B349**, 597 (1995); K.G. Chetyrkin, J.H. Kühn, M. Steinhauser, *Phys. Lett.* **B351**, 331 (1995).

- [14] A. Sirlin, *Phys. Rev.* **22**, 971 (1980); W.J. Marciano, A. Sirlin, *Phys. Rev.* **22**, 2695 (1980).
- [15] W.J. Marciano, *Phys. Rev.* **D20**, 274 (1979).
- [16] M. Consoli, W. Hollik, F. Jegerlehner, *Phys. Lett.* **B227**, 167 (1989).
- [17] A. Djouadi, *Nuovo Cim.* **A100**, 357 (1988); D. Yu. Bardin, A.V. Chizhov, Dubna preprint E2-89-525 (1989); B.A. Kniehl, *Nucl. Phys.* **B347**, 86 (1990); F. Halzen, B.A. Kniehl, *Nucl. Phys.* **B353**, 567 (1991); A. Djouadi, P. Gambino, *Phys. Rev.* **D49**, 3499 (1994).
- [18] B.A. Kniehl, J.H. Kühn, R.G. Stuart, *Phys. Lett.* **B214**, 621 (1988); B.A. Kniehl, A. Sirlin, *Nucl. Phys.* **B371**, 141 (1992); *Phys. Rev.* **D47**, 883 (1993); S. Fanchiotti, B.A. Kniehl, A. Sirlin, *Phys. Rev.* **D48**, 307 (1993).
- [19] A. Sirlin, *Phys. Rev.* **D29**, 89 (1984).
- [20] For a review see: K.G. Chetyrkin, J.H. Kühn, A. Kwiatkowski, in [5], p. 175
- [21] B.A. Kniehl, in [5], p. 299
- [22] D. Bardin *et al.*, in [5], p. 7
- [23] G. Degrassi, P. Gambino, A. Vicini, hep-ph/9603374; P. Gambino, MPI-PhT-96-77; MPI-PhT-96-85.
- [24] A.A. Akhundov, D.Yu. Bardin, T. Riemann, *Nucl. Phys.* **B276**, 1 (1986); W. Beenakker, W. Hollik, *Z. Phys.* **C40**, 141 (1988); J. Bernabeu, A. Pich, A. Santamaria, *Phys. Lett.* **B200**, 569 (1988);
- [25] A. Denner, W. Hollik, B. Lampe, *Z. Phys.* **C60**, 193 (1993).
- [26] J. Fleischer, F. Jegerlehner, P. Rączka, O.V. Tarasov, *Phys. Lett.* **B293**, 437 (1992); G. Buchalla, A.J. Buras, *Nucl. Phys.* **B398**, 285 (1993); G. Degrassi, *Nucl. Phys.* **B407**, 271 (1993); K.G. Chetyrkin, A. Kwiatkowski, M. Steinhauser, *Mod. Phys. Lett.* **A8**, 2785 (1993).
- [27] A. Kwiatkowski, M. Steinhauser, *Phys. Lett.* **B344**, 359 (1995); S. Peris, A. Santamaria, CERN-TH-95-21 (1995).
- [28] K.G. Chetyrkin, A.L. Kataev, F.V. Tkachov, *Phys. Lett.* **B85**, 277 (1979); M. Dine, J. Sapirstein, *Phys. Rev. Lett.* **43**, 668 (1979); W. Celmaster, R. Gonsalves, *Phys. Rev. Lett.* **44**, 560 (1980); S.G. Gorishny, A.L. Kataev, S.A. Larin, *Phys. Lett.* **B259**, 144 (1991); L.R. Surguladze, M.A. Samuel, *Phys. Rev. Lett.* **66**, 560 (1991); A. Kataev, *Phys. Lett.* **B287**, 209 (1992).
- [29] T.H. Chang, K.J.F. Gaemers, W.L. van Neerven, *Nucl. Phys.* **B202**, 407 (1982); J.H. Kühn, B.A. Kniehl, *Phys. Lett.* **B224**, 229 (1990); *Nucl. Phys.* **B329**, 547 (1990); K.G. Chetyrkin, J.H. Kühn, *Phys. Lett.* **B248**, 359 (1992); K.G. Chetyrkin, J.H. Kühn, A. Kwiatkowski, *Phys. Lett.* **B282**, 221 (1992); K.G. Chetyrkin, A. Kwiatkowski, *Phys. Lett.* **B305**, 285 (1993); Karlsruhe preprint TTP93-24 (1993); K.G. Chetyrkin, Karlsruhe preprint TTP93-5 (1993); K.G. Chetyrkin, J.H. Kühn, A. Kwiatkowski, in [7], p. 175; S. Larin,

- T. van Ritbergen, J.A.M. Vermaseren, *ibidem*, p. 265; *Phys. Lett.* **B320**, 159 (1994).
- [30] S. Bethke, in: Proceedings of the Tennessee International Symposium on Radiative Corrections, Gatlinburg 1994, Ed. B.F.L. Ward, World Scientific 1995.
- [31] E. Torrence (SLD Coll.), ICHEP96 (talk), Warsaw, July 1996.
- [32] K. McFarlane (CCFR Coll.), ICHEP96 (talk), Warsaw, July 1996.
- [33] W. de Boer, A. Dabelstein, W. Hollik, W. Möhle, U. Schwickerath, hep-ph/9609209.
- [34] M. Grünewald, ICHEP96 (talk), Warsaw, July 1996.
- [35] J. Ellis, G.L. Fogli, E. Lisi, hep-ph/9608329.
- [36] G. Passarino, talk at CRAD96, Cracow, August 1996; S. Dittmaier, D. Schildknecht, hep-ph/9609488.
- [37] P. Chankowski, S. Pokorski, hep-ph/9509207; J. Ellis, G.L. Fogli, E. Lisi, *Z. Phys.* **C69**, 627 (1996); S. Dittmaier, D. Schildknecht, G. Weiglein, hep-ph/9602436; G. Passarino, hep-ph/9604344.
- [38] A. Denner, R. Guth, W. Hollik, J.H. Kühn, *Z. Phys.* **C51**, 695 (1991); J. Rosiek, *Phys. Lett.* **B252**, 135 (1990); M. Boulware, D. Finnell, *Phys. Rev.* **D44**, 2054 (1991).
- [39] G. Altarelli, R. Barbieri, F. Caravaglios, CERN-TH.7536/94 (1994); C.S. Lee, B.Q. Hu, J.H. Yang, Z.Y. Fang, *J. Phys. G* **19**, 13 (1993); Q. Hu, J.M. Yang, C.S. Li, *Comm. Theor. Phys.* **20**, 213 (1993); J.D. Wells, C. Kolda, G.L. Kane, *Phys. Lett.* **B338**, 219 (1994); G.L. Kane, R.G. Stuart, J.D. Wells, *Phys. Lett.* **B354**, 350 (1995); M. Drees *et al.*, hep-ph/9605447
- [40] P. Chankowski, A. Dabelstein, W. Hollik, W. Möhle, S. Pokorski, J. Rosiek, *Nucl. Phys.* **B417**, 101 (1994); D. Garcia, J. Solà, *Mod. Phys. Lett.* **A9**, 211 (1994).
- [41] D. Garcia, R. Jiménez, J. Solà, *Phys. Lett.* **B347** (1995) 309; **347**, 321 (1995); D. Garcia, J. Solà, *Phys. Lett.* **B357**, 349 (1995); A. Dabelstein, W. Hollik, W. Möhle, in *Perspectives for Electroweak Interactions in e^+e^- Collisions*, Ringberg Castle 1995, Ed. B.A. Kniehl, World Scientific 1995, p. 345; P. Chankowski, S. Pokorski, hep-ph/9603310.
- [42] J. Ellis, G. Ridolfi, F. Zwirner, *Phys. Lett.* **B257**, 83 (1991).
- [43] H.P. Nilles, *Phys. Rep.* **110**, 1 (1984); H.E. Haber, G. Kane, *Phys. Rep.* **117**, 75 (1985); J.F. Gunion, H.E. Haber, *Nucl. Phys.* **B272**, 1 (1986); *Nucl. Phys.* **B402**, 567 (1993); J.F. Gunion, H.E. Haber, G. Kane, S. Dawson, *The Higgs Hunter's Guide*, Addison-Wesley, 1990.
- [44] R. Barbieri, G. Gamberini, G. Giudice, G. Ridolfi, *Nucl. Phys.* **B296**, 75 (1988).

- [45] R. Barbieri, G. Giudice, *Phys. Lett.* **B309**, 86 (1993); R. Garisto, J.N. Ng, *Phys. Lett.* **B315**, 372 (1993); S. Bertolini, F. Borzumati, A. Masiero, G. Ridolfi, *Nucl. Phys.* **B353**, 591 (1991) and references therein; N. Oshimo, *Nucl. Phys.* **B404**, 20 (1993); S. Bertolini, F. Vissani, *Z. Phys.* **C67**, 513 (1995).
- [46] CLEO-Collaboration, R. Ammar *et al.*, *Phys. Rev. Lett.* **74**, 2885 (1995).
- [47] ALEPH Collaboration, CERN-PPE/96-10; OPAL Collaboration, CERN-PPE/96-019; CERN-PPE/96-020; DELPHI Collaboration, CERN-PPE/96-75; D0 Collaboration, *Phys. Rev. Lett.* **76**, 2222 (1996); FERMILAB-PUB-95/380-E; ALEPH Collaboration, CERN PPE/96-079.
- [48] *Particles and Fields*, *Phys. Rev.* **D50**, 1173 (1994); R.M. Barnett *et al.*, *Phys. Rev.* **D54**, 1 (1996).
- [49] W. de Boer *et al.*, hep-ph/9603346 and references therein.
- [50] M. Schmelling, Plenary talk at 28th Int. Conf. on High Energy Physics, Warsaw, July, 1996.